Initial State Dependence of Low-Energy Electron Emission in Fast Ion Atom Collisions

R. Moshammer,[1,*] P. D. Fainstein,[2] M. Schulz,[4,1] W. Schmitt,[1] H. Kollmus,[1] R. Mann,[3] S. Hagmann,[5] and J. Ullrich[1]
[1]*Universität Freiburg, Hermann-Herder-Strasse 3, 79104 Freiburg, Germany*
[2]*Centro Atomico Bariloche, Comisión Nacional de Energía Atómica, 8400 Bariloche, Argentina*
[3]*Gesellschaft für Schwerionenforschung, 64220 Darmstadt, Germany*
[4]*Department of Physics, University of Missouri-Rolla, Rolla, Missouri 65409*
[5]*Department of Physics, Kansas State University, Manhattan, Kansas 66506-2501*
(Received 24 May 1999)

Single and multiple ionization of neon and argon atoms by 3.6 MeV/u Au^{53+} impact has been explored in kinematically complete experiments. Doubly differential cross sections for low-energy electron emission have been obtained for a defined charge state of the recoiling target ion and the receding projectile. Observed target specific structures in the electron continuum are attributable to the nodal structure of the initial bound state momentum distribution. The experimental data are in excellent accord with continuum-distorted-wave eikonal-initial-state single ionization calculations if multiple ionization is considered appropriately.

PACS numbers: 34.10.+x, 34.50.Fa

In a series of recent publications [1–3] on double ionization of helium the old question was revitalized whether the correlated ground state wave function of many-electron atoms or molecules is directly accessible in any practicable experiment [4]. Whereas the mapping of effective one-electron initial-state momentum distributions (Compton profiles) by impulsive binary collisions with fast electrons has become a well-established technique in kinematically complete $(e, 2e)$ experiments (see, e.g., [5]), such measurements are a hopeless task for correlated many-electron states. The simultaneous detection of several low-energy electrons emitted after interaction of fast heavy ions with atoms or molecules has been proposed as an alternative approach. Evidence was provided that the emitted electrons should map the correlated momenta of the initial state [3,6]. However, the interpretation strongly depends on theoretical models used [1], and up to now it has not even been conclusively demonstrated for single ionization that the low-energy electron continuum depends on the initial-state wave function in a characteristic way.

Low-energy electrons are produced in collisions where the energy transferred to the target is just slightly above the ionization threshold. Thus, according to classical (Wannier) or semiclassical threshold theories [7] it was generally assumed that the low-energy continuum is insensitive on the initial state. This "loss of memory" of initial conditions is in agreement with the accepted interpretation of double photoionization measurements close to the ionization threshold [2], and it is in accord with low-energy electron impact ionization experiments where both the scattered and the ionized electron escape with very low energies [8]. However, results of continuum-distorted-wave eikonal-initial-state (CDW-EIS) calculations predict the emission of low-energy electrons in fast ion induced ionization to depend on the details of the target potential [9]. Moreover, it was predicted more than 15 years ago that the shape of the "cusp peak" after projectile ionization (electron loss to the continuum, ELC), i.e., low-energy electrons in the projectile frame, mirrors the nodal structure of the initial state and the alignment of the target with respect to the beam axis [10]. These calculations have never been verified experimentally.

After decades of systematic electron spectroscopy in ion atom collisions there are only a very few experimental data sets of doubly differential cross sections (DDCS) for targets heavier than helium [11–13], and, to the best of our knowledge, there are no studies that cover the electron energy range from some 10 eV down to zero kinetic energy. Such data are extremely difficult to collect with conventional spectrometers because of the large uncertainties of usually up to 50% for electron energies below a few eV [14–16]. Thus, the low-energy part of the electron spectrum is basically unexplored even though it strongly contributes to the total ionization cross section. Moreover, a reliable experimental test of single ionization theories in the nonperturbative regime (i.e., at large projectile charge to projectile velocity ratio q/v_p) was missing because it was impossible to unambiguously separate pure single ionization from multielectron transitions. Only the recent development of entirely new and extremely efficient electron spectrometers combined with recoil-ion momentum spectroscopy [17] made such experiments feasible.

In this Letter we report on the first observation of distinct target specific structures in the low-energy electron continuum after ionization of Ne and Ar atoms in collisions with 3.6 MeV/u Au^{53+}. The DDCS for electron energies from 100 eV down to $E_e = 0$ eV have been measured in coincidence with the full momentum vector and the charge state of the recoiling target ion and the charge state of the outgoing projectile (no charge exchange). In this way the DDCS for well-defined degrees of ionization have been obtained. The experimental data are in accord with state of the art CDW-EIS calculations

considering the long-range Coulomb interaction with the projectile in the initial and in the final state.

The experiments were performed at the Universal Accelerator (UNILAC) of GSI (Gesellschaft für Schwerionenforschung) using our multielectron recoil-ion momentum spectrometer. Details about the operating principle and the resolution of the spectrometer have been reported previously [18]. Briefly, a collimated (0.5 mm diameter) and charge state selected beam of 3.6 MeV/u Au^{53+} ions is crossed with a supersonic beam (2.8 mm diameter) of Ne and Ar, respectively. Electrons and target ions produced in the collision zone are extracted into opposite directions by a weak 1.36 V/cm electric field acting over 22 cm along the ion-beam (longitudinal) direction. An additional solenoidal magnetic field between 6.1 and 20.5 G (high and low resolution modes, respectively) confines the electrons transverse motion. This way all electrons with transverse energies below 115 eV and all recoil ions are projected onto position sensitive multihit detectors. The recoil-ion charge state and the full momentum vector of both, recoil-ion and electron, are calculated from their measured absolute flight times and their positions on the detectors. The outgoing projectile is charge state analyzed after the collision chamber and detected by a fast scintillator in coincidence with the target fragments. In the high resolution mode an optimum electron momentum resolution of $\Delta v_{\parallel} = 1 \times 10^{-2}$ a.u. in the longitudinal direction and $\Delta v_{\perp} = 1.4 \times 10^{-2}$ a.u. in the transverse direction has been achieved. This corresponds to an electron energy resolution of $\Delta E_e = 2.5$ meV for electron energies $E_e = 0$ eV. The systematic uncertainty in the determination of the electron energy is estimated to be smaller than $\pm 5\%$. For the calibration of the origin $E_e = 0$ eV an accuracy of ± 1 meV has been obtained. The efficiency of the spectrometer is constant over the whole energy range and the determination of relative cross sections is limited by statistical errors only. Electron spectra coincident with single up to sixfold ionization of Ne and up to eightfold ionization of Ar have been obtained. Since for each event the momentum vectors of up to three electrons were recorded the experimental data are kinematically complete for single, double, and triple ionization. The momentum balance between all collision partners as well as low-energy electron spectra as functions of the momentum transfer will be discussed in a subsequent publication.

The experimental data are compared with results obtained with an extended CDW-EIS model, where the initial bound and the final continuum state is calculated numerically by solving the time-dependent Schrödinger equation with a Hartree-Fock-Slater model potential [19]. This first order theory has been impressively demonstrated to be valid far beyond the Bethe-Born approximation for various charged projectiles (protons, antiprotons, and highly charged ions) over a large range of perturbation strengths [20].

Selected cuts on the experimental doubly differential cross section for electron emission in coincidence with pure single ionization of Ne are shown in Fig. 1 in comparison with CDW-EIS results. Cylindrical coordinates in velocity space are chosen in accordance with recent studies on low-energy electron emission from He targets [21] and in accordance with the commonly used representation of ELC electrons [10]. In order to account for the increasing volume element with increasing $v_{\perp}$ the presented DDCS are defined as DDCS $= d^2\sigma/(dv_{\parallel} dv_{\perp} 2\pi v_{\perp})$. The experimental single ionization data were normalized to the total CDW-EIS cross sections for Ne and Ar, respectively. The accuracy of various differential cross section cuts relative to each other is limited only by the statistical errors.

The experimental and theoretical distributions exhibit characteristic features and some of them have been discussed before. For example, the preferential forward emission of electrons has been attributed to the postcollision interaction [16,22]. The emerging highly charged projectile drags the electrons into the forward direction. Furthermore, a peak, the recently reported "target cusp," appears at ultralow electron energies [21]. In the limit $v \to 0$ the cross section differential in electron velocity diverges like $d\sigma/dv = 1/v$ for a Coulomb potential mainly as a consequence of pure phase space arguments [10].

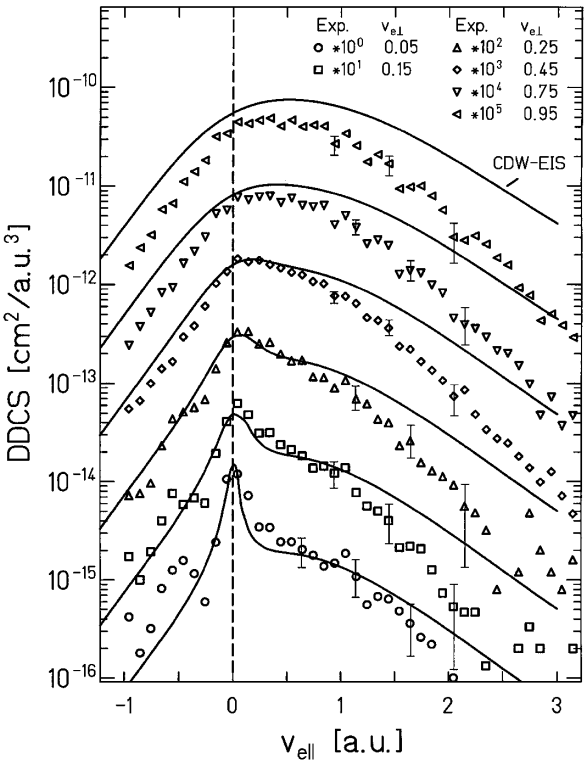

FIG. 1. Doubly differential cross sections DDCS $= d^2\sigma/(dv_{\parallel} dv_{\perp} 2\pi v_{\perp})$ as functions of the longitudinal electron velocity for certain transverse velocity cuts in pure singly ionizing 3.6 MeV/u Au^{53+} on Ne collisions. DDCS at different $v_{\perp}$ are multiplied by factors of 10, respectively. Lines: theoretical CDW-EIS results.

Beyond these well established features, however, especially for the Ar target distinct structures emerge which are beyond the statistical fluctuations (Fig. 2). Already the total widths of the distributions are much narrower than for the Ne target. As will be discussed in detail below exactly these patterns will turn out to be signatures of the initial-state wave function. First, the overall comparison with the CDW-EIS calculation is discussed. Systematic discrepancies are observed only at higher electron energies. In the "single active electron" theory the whole impact parameter range only and exclusively contributes to single ionization. But, particularly at small impact parameters, single ionization is competing with double and multiple ionization. This close collision contribution can approximately be included by taking the sum of the experimental DDCS over several recoil-ion charge states, i.e., by plotting the DDCS irrespective of the degree of ionization (Fig. 3). This quantity is the one measured by conventional electron spectroscopy. The considerably improved agreement in shape between experiment and theory over the whole range of electron energies and for both targets supports our interpretation. It further demonstrates that reliable ionization data are obtainable only when the charge state of the remaining target ion is known in the experiment.

Much more pronounced than in the Ne case, systematic structures appear in the calculated and in the measured electron spectra of Ar, particularly for the small transverse velocity cuts. In order to elucidate the origin of these humps and dips several calculations have been performed to determine the contribution to the DDCS of selected target states. According to these calculations ionization of electrons from the argon $3p$ state amounts to more than 90% to the total cross section. Inspection of the contribution of the $3p_0$ and $3p_1$ magnetic substates reveals striking differences in the shapes of the electron spectra (Fig. 4). Surprisingly, ionization of the $3p_0$ state dominantly contributes to the cross section though it is occupied with only two electrons in comparison with four electrons in the $3p_1$ state. This is true particularly if continuum electrons with large longitudinal momenta are considered. According to theory the same structure appears also in the perturbative regime like, e.g., for MeV protons.

Therefore, the observed structure in the electron spectra is a property of the target which can be associated to the nodes and maxima of the target density distribution in momentum space. For example, the squared Ar $3p_0$ wave function in momentum space is aligned along the ion-beam direction with maxima at longitudinal momenta of around ± 0.5 and ± 1.6 a.u. and a node in between. The positions of these maxima coincide with the positions of the humps in the continuum momentum distributions (Fig. 4).

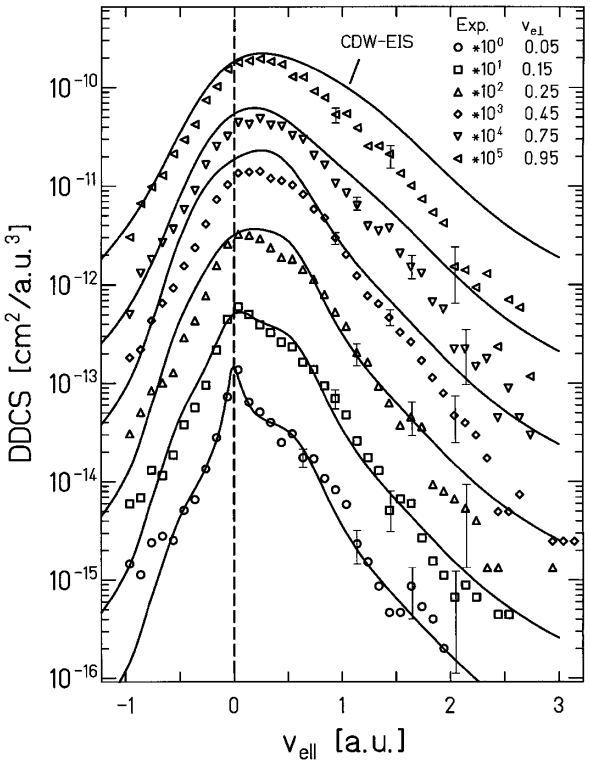

FIG. 2. Same as Fig. 1 for 3.6 MeV/u Au^{53+} on Ar collisions.

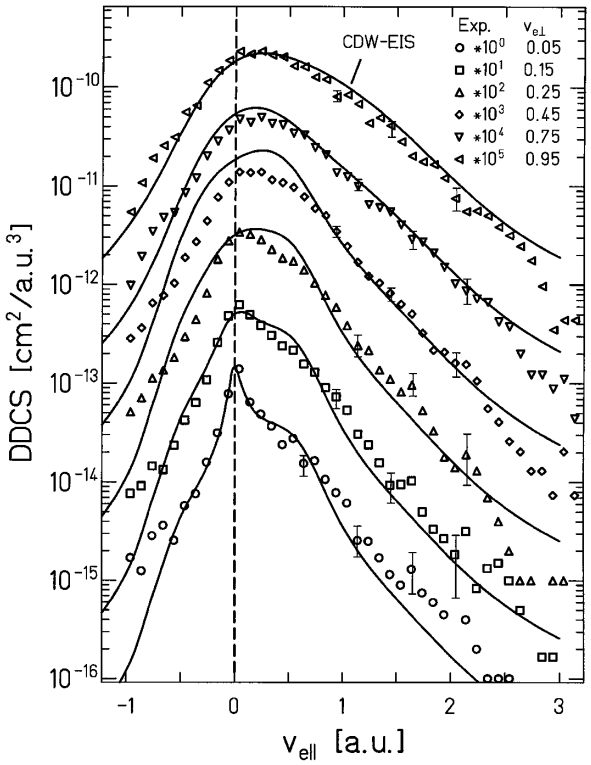

FIG. 3. Doubly differential cross section for electron emission due to single, double, or triple ionization of Ar. The DDCS for the specified recoil-ion charge states are added according to their relative contribution to the total cross section. The experimental data are divided by 1.4.

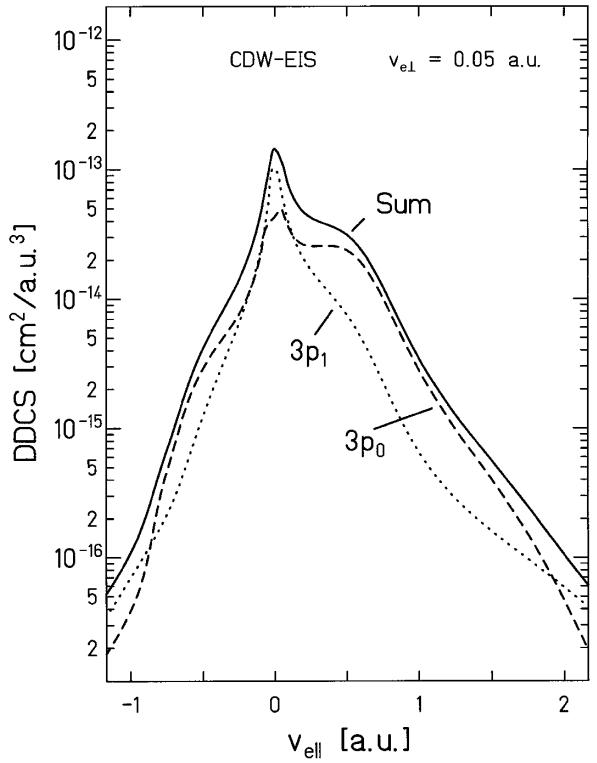

FIG. 4. Doubly differential CDW-EIS cross section at $v_\perp = 0.05$ a.u. for ionization of Ar $3p$ electrons only and the contributions of magnetic $m = 0$ $(3p_0)$ and $m = \pm 1$ $(3p_1)$ substates. The quantization axis is the beam axis (longitudinal direction).

Moreover, since the $3p_1$ state is aligned perpendicular to the ion-beam direction, the projection of this initial-state momentum distribution onto the longitudinal axis yields a considerably narrower distribution. This reduced width is also manifested in the calculated momentum distribution. The remaining discrepancy between theory and experiment (see Fig. 3) might be a result of using still too simplified target wave functions in the calculations.

In summary, we have experimentally mapped the low-energy electron continuum of Ne and Ar targets for well-defined degrees of ionization. Very good agreement with the most elaborate theory available is obtained if multiple ionization channels are approximately accounted for. Distinct structures, experimentally observed for the first time, can be related to the initial-state momentum distribution. Our results conclusively support the previously developed simple physical picture that ionization by fast ions can be viewed as weighted "projection" of the bound state to the low-lying continuum. Since the momentum transfer is very small and almost purely transversal, the final longitudinal momentum distribution is an "image" of the nodal structure of the initial bound state momentum distribution. In future improved multiple ionization experiments might lead to a powerful method for the study of correlated many-electron bound states of atoms, molecules, and clusters.

We acknowledge support from GSI, NSF, DOE, and the Deutsche Forschungsgemeinschaft within the SFB 276 and the Leibniz-program. P. F. is grateful for the hospitality of the University of Freiburg and acknowledges support from Fundación Antorchas. We are grateful to V. Schmidt for numerous discussions.

*Email address: Moshammer@physik.uni-freiburg.de

[1] S. Keller, H. J. Lüdde, and R. M. Dreizler, Phys. Rev. A **55**, 4215 (1997); S. Keller *et al.* (to be published).
[2] R. Dörner *et al.*, Phys. Rev. A **57**, 1074 (1998).
[3] R. Moshammer *et al.*, Phys. Rev. Lett. **77**, 1242 (1996).
[4] W. Heisenberg, Z. Phys. **43**, 172 (1927).
[5] I. E. McCarthy and E. Weigold, Rep. Prog. Phys. **54**, 789 (1991).
[6] B. Bapat *et al.*, J. Phys. B **32**, 1859 (1999).
[7] J. M. Rost, J. Phys. B **27**, 5923 (1994).
[8] M. Kelley, W. T. Rogers, R. J. Celotta, and S. R. Mielczarek, Phys. Rev. Lett. **51**, 2191 (1983).
[9] P. D. Fainstein, L. Gulyás, F. Martín, and A. Salin, Phys. Rev. A **53**, 3243 (1996).
[10] J. Burgdörfer, Phys. Rev. Lett. **51**, 374 (1983).
[11] M. E. Rudd, L. H. Toburen, and N. Stolterfoht, At. Data Nucl. Data Tables **18**, 413 (1976).
[12] N. Stolterfoht *et al.*, Phys. Rev. Lett. **80**, 4649 (1998).
[13] S. Suárez *et al.*, Phys. Rev. A **48**, 4339 (1993).
[14] L. C. Tribedi *et al.*, Phys. Rev. A **54**, 2154 (1996).
[15] M. E. Rudd, Y. K. Kim, D. H. Madison, and T. J. Gay, Rev. Mod. Phys. **64**, 441 (1992).
[16] N. Stolterfoht, R. D. DuBois, and R. D. Rivarola, *Electron Emission in Heavy-Ion Atom Collisions*, edited by J. P. Toennies (Springer-Verlag, Berlin, 1997), Vol. 20.
[17] J. Ullrich *et al.*, J. Phys. B **30**, 2917 (1997).
[18] R. Moshammer *et al.*, Nucl. Instrum. Methods Phys. Res., Sect. B **108**, 425 (1996).
[19] L. Gulyás, P. D. Fainstein, and A. Salin, J. Phys. B **28**, 245 (1995).
[20] N. Stolterfoht *et al.*, Phys. Rev. A **52**, 3796 (1995).
[21] W. Schmitt *et al.*, Phys. Rev. Lett. **81**, 4337 (1998).
[22] R. Moshammer *et al.*, Phys. Rev. Lett. **73**, 3371 (1994).